NASA TECHNICAL MEMORANDUM

GASEOUS EXHAUST EMISSIONS FROM A J-58 ENGINE AT SIMULATED SUPERSONIC FLIGHT CONDITIONS

by James D. Holdeman
Lewis Research Center
Cleveland, Ohio 44135
April 1974

ABSTRACT

Emissions of total oxides of nitrogen, unburned hydrocarbons, carbon monoxide, and carbon dioxide from a J-58 engine at simulated flight conditions of Mach 2.0, 2.4, and 2.8 at 19.8 km altitude are reported. For each flight condition, measurements were made for four engine power levels from maximum power without afterburning through maximum afterburning. These measurements were made 7 cm downstream of the engine primary nozzle using a single point traversing gas sample probe. Results show that emissions vary with flight speed, engine power level, and with radial position across the exhaust.

GASEOUS EXHAUST EMISSIONS FROM A J-58 ENGINE AT

SIMULATED SUPERSONIC FLIGHT CONDITIONS

by James D. Holdeman
Lewis Research Center

SUMMARY

Emissions of total oxides of nitrogen, unburned hydrocarbons, carbon monoxide, and carbon dioxide from a J-58 engine at simulated flight conditions of Mach 2.0, 2.4, and 2.8 at 19.8 km altitude are reported. For each flight condition, detailed emissions and temperature measurements were made for four engine power levels from maximum power without afterburning through maximum afterburning. These measurements were made on a single diameter 7 cm downstream of the engine primary nozzle using a single point traversing gas sample probe. Emission profiles, presented in terms of concentration (ppmv) and local emission index (g emittant/kg fuel), show that emissions vary with flight speed, engine power level, and with radial position across the exhaust.

INTRODUCTION

Testing of a J-58 afterburning turbojet engine was conducted to determine its emissions of oxides of nitrogen, unburned hydrocarbons, carbon monoxide, and carbon dioxide, at simulated supersonic, high altitude flight conditions.

Emission measurements from aircraft turbine engines, and in particular, afterburning engines, at high altitude supersonic flight conditions are relevant to answering questions about the environmental impact of the supersonic transport. The purpose of the present investigation is to provide an emissions calibration for the J-58 engine for subsequent use in the NASA Stratosphere Jet Wake Flight Experiment (discussed in ref. 1). In this program, in-flight sampling of exhaust constituents will be made in the wake of a YF-12 aircraft, powered by two J-58 engines, during supersonic, stratospheric flight. The emissions calibration tests will provide the initial conditions for assessing the dispersion and dilution of exhaust products in the stratosphere. In addition, these tests will add to the general knowledge about emissions from afterburning turbojet engines at high altitude conditions. Although emission levels for the J-58 engine may not necessarily be representative of emissions from engines designed for present or future commercial supersonic aircraft, the trends should be similar.

Previous studies dealing with aircraft jet engine emissions at altitude conditions are reported in references 2 to 6. In these, various engines and flight conditions have been examined. The J-93 tests (ref. 6) conducted at AEDC as part of the Climatic Impact Assessment Program are

the most closely related to the present investigation in terms of the size of the engine tested and flight conditions examined.

The present investigation was conducted in the Propulsion Systems Laboratory at the Lewis Research Center. Test conditions included simulated flight speeds of Mach 2.0, 2.4, and 2.8, all at 19.8 km altitude. At each flight condition, data traverses across the diameter of the primary exhaust nozzle were made for four engine power levels from maximum power without afterburning to maximum afterburning.

APPARATUS

Engine

The J-58 engine is an afterburning turbojet designed for operation at flight speeds in excess of Mach 2 at stratospheric altitudes. Two of these engines provide the propulsion for the NASA/USAF YF-12A aircraft. The J-58 engine tested in this program is one of two that will be used in the NASA Stratosphere Jet Wake Experiment.

Facility

The engine was tested in the Propulsion Systems Laboratory at the Lewis Research Center. This altitude chamber facility and associated air handling equipment provided conditioned inlet airflow and appropriate exhaust pressure to accurately simulate the conditions at the engine inlet and exhaust corresponding to the selected supersonic flight conditions. The engine operates using JP-7 fuel. This fuel was heated to 395 K prior to entering the engine to simulate the condition aboard the aircraft during supersonic flight.

Gas Sample Probe and Transport System

A single point, traversing, water-cooled gas sample probe was used to obtain emission measurements. The probe and its traversing mechanism are shown mounted behind the engine in figure 1(a). The traversing mechanism had the capability to translate the probe ±60 cm horizontally and ±20 cm vertically from the engine centerline.

The sensor area of the probe is shown in figure 1(b). A total pressure sensor was mounted 2.5 cm above the sample probe and three unshielded iridium/iridium-rhodium thermocouples were mounted 2.5 and 5 cm below and 5 cm above the gas sample probe. The gas sample sensor had an i.d. of 0.717 cm. The probe tip extended 1.9 cm forward of the rake body. This section was water-cooled for a distance of 8 cm downstream from the tip both for sample conditioning and probe integrity. Following this section, the sample line increased to 0.818 cm i.d. (3/8 in. o.d.). For afterburning conditions, a second water-cooled heat exchanger on the next 30 cm of

line was used to provide additional quenching of the sample. Approximately 10 meters of 0.95 cm stainless-steel line was used to transport the sample to the analyzers. In order to prevent condensation of water and to minimize adsorbtion-desorbtion effects of hydrocarbon compounds, the line was heated with steam at 428 K. Four heated metal bellows pumps (two pumps in series in each of two parallel legs) were used to supply sufficient gas sample pressure, 17 N/cm^2, to operate the analytical instruments. The gas sample line residence time was less than 2 seconds for all test conditions.

Gas Analysis Instrumentation

The exhaust gas analysis system, figure 2, is a packaged unit consisting of four commercially available instruments along with associated peripheral equipment necessary for sample conditioning and instrument calibration. In addition to the visual readout at the console, electrical inputs are provided to the facility computer for on-line analysis and data evaluation.

The hydrocarbon content of the exhaust gas was measured on a wet basis using a Beckman Instruments Model 402 Hydrocarbon Analyzer. This instrument is of the flame ionization detector type. The concentration of the oxides of nitrogen was measured on a dry basis using a Thermo Electron Corporation Model 10A Chemiluminescence Analyzer. This instrument includes a thermal converter to reduce NO_2 to NO. Data were obtained as total NO_X ($NO + NO_2$). Both carbon monoxide and carbon dioxide were measured dry using analyzers of the nondispersive infrared (NDIR) type. These instruments were Beckman Instruments Model 315B.

TEST CONDITIONS AND PROCEDURE

The engine test conditions are presented in table I. Engine inlet air was conditioned to correspond to the values at the engine face for supersonic flight speeds of Mach 2.0, 2.4, and 2.8 at an altitude of 19.8 kilometers. For each flight condition, tests were made at four engine power settings from military through maximum afterburning, see table I. The altitude chamber pressure for each flight condition was selected to ensure a hard choke at the engine primary exhaust nozzle. Note that the altitude chamber pressure does not need to be equal to the ambient static pressure for the simulated altitude. The internal performance of the engine is correctly simulated for all pressures low enough to choke the nozzle.

Emission traverses were made at the plane of the primary nozzle (actually the probe was 6.7 cm from the exit plane when the engine was cold with the nozzle wide open). Data were obtained at 5 cm (nominal) intervals across the horizontal exhaust diameter resulting in approximately 20 data points per traverse. These small increments were necessary to document the steep gradients in emissions and temperature found in after-

burning operation. The interval was increased to nominally 7.5 cm for military power tests since emissions and temperature gradients at this condition were much less than for afterburning conditions. The time required for each traverse varied from 30 to 45 minutes. Complete surveys (four power levels at each flight condition required approximately four hours of continuous engine operation.

At the Mach 2.0 condition limited data were obtained up to 20 cm above and below the engine centerline on the vertical diameter. These data showed variations similar to those on the horizontal diameter.

All gas analysis instruments were checked for zero and span prior to each traverse. Because the console allows rapid selection of zero, span, or sample modes, these frequent checks could be made during power level changes while the engine was running.

Concentrations which were measured on a dry basis (NO_x, CO, and CO_2) are reported on a wet basis, correcting for water vapor, including both inlet air humidity and water vapor from combustion. The relations used are given in reference 7.

Emission levels of all constituents were converted to emission index (EI) parameters based on the local (gas sample) fuel-air ratio according to the relations given in reference 7.

RESULTS AND DISCUSSION

The emissions and temperature profile data obtained during the test program are presented in figures 3 to 11. Measured exhaust total temperatures are shown in figure 3. In this figure and all subsequent ones, the horizontal axis on the figures is the radial distance from the engine centerline nondimensionalized by the calculated exit radius (R_8) at each condition. This radius varies with flight condition and engine power level. Data for the Mach 2.0 flight condition is shown in part (a) of the figure, data for Mach 2.4 is shown in part (b), and data for Mach 2.8 is shown in part (c). In all cases the simulated flight altitude is 19.8 kilometers. For each flight condition, data is shown for four engine power levels; military (maximum power without afterburning), minimum afterburning (Min A/B), an intermediate afterburning power level (Int A/B), and maximum afterburning (Max A/B), see table I. For all flight conditions the temperature is quite uniform across the exhaust plane at military power, but significant temperature gradients exist across the diameter in the afterburning modes. Each data point shown is the average of the readings from the three thermocouples. No radiation correction was applied to the measured temperatures.

The local fuel-air ratios (f/a) calculated from the gas sample measurements are shown in figure 4(a), (b), and (c) for Mach 2.0, 2.4, and 2.8, respectively. For each flight condition the measured overall fuel-air ratios are listed adjacent to the symbol designations. These are in

excellent correspondence to the averaged local fuel-air ratios obtained from the gas sample.

Emissions data for the oxides of nitrogen, carbon monoxide, and unburned hydrocarbons are presented both in terms of volumetric concentrations (ppmv) and emission index (g emittant/kg fuel). Because the fuel air ratio for each power level at each flight condition varies across the exhaust diameter, the emission index profile is not a constant times the corresponding concentration profile.

Oxides of Nitrogen Emissions

The volumetric exhaust concentration of the oxides of nitrogen for each of the conditions are shown in figure 5. NO_x concentrations at military power are nearly uniform across the exhaust, with an increase of about a factor of 2 indicated in going from Mach 2.0 to 2.8. In afterburning modes, significant gradients in NO_x are observed across the exhaust for all conditions. The values shown are total NO_x ($NO + NO_2$) for all conditions except maximum afterburning at Mach 2.4. At this condition the converter on the chemiluminescence instrument was inadvertently turned off, thus the values shown represent NO only for this condition.

For all conditions except maximum afterburning at Mach 2.8, the measured NO_x on the engine centerline is less in afterburning than at the corresponding military power level. For all conditions the NO_x concentration at mid-radius (downstream of the afterburner flame holders) is greater than that at the same radius at military power. From figures 3, 4, and 5 it can be seen that the NO_x concentration, the exhaust temperature, and the local fuel air ratio curves have the same shape. Thus it is not surprising that the local emission index profiles for NO_x in figure 6 are much more uniform than the concentration profiles since the emission index is inversely proportional to the fuel-air ratio for a given volumetric concentration. For all afterburning conditions the NO_x emission index profiles decrease toward the engine centerline. For each flight condition the emission indices in the afterburning modes are on the order of one-half of the value at military power for the same flight conditions. The emission indices at military power show that the oxides of nitrogen emissions increase by slightly more than a factor of two from Mach 2.0 to 2.8. The emission index values for military power at Mach 2.4 further suggest that the increase in linear with Mach number is this range.

Unburned Hydrocarbon Emissions

Exhaust concentrations of unburned hydrocarbons, as ppm C (parts per million carbon by volume), are shown in figure 7(a), (b), and (c) for Mach 2.0, 2.4, and 2.8, respectively. For all flight conditions, at military power, unburned hydrocarbons were measured at less than 10 ppm C, corresponding to emission indices, see fig. 8, of less than 0.3.

For minimum afterburning, at all flight speeds, unburned hydrocarbon concentrations on the order of 10 000 ppm C were observed on the engine centerline. However, for these conditions, the measured concentrations at radii greater than $R_8/2$ was at least two orders of magnitude less than the centerline value. The gradient in the emission indices is even greater than this since high hydrocarbon concentrations occur at radii where the local fuel-air ratio is lowest and conversely low hydrocarbon concentrations occur at radii where the local fuel-air ratio is highest; see figures 4, 7, and 8.

For the Mach 2.0 condition, high centerline hydrocarbon concentrations are observed for all afterburner power levels, but the width of the zone decreases with increasing power. Because the fuel-air ratio increases substantially as power level increases, the centerline emission index decreases, see fig. 8(a).

For both Mach 2.4 and 2.8, the centerline concentration of unburned hydrocarbons decreases with increasing power, and consequently the emission indices decrease even more rapidly. Note that at both intermediate and maximum afterburning, unburned hydrocarbon emission decrease significantly from Mach 2.0 to 2.8. For maximum afterburning at Mach 2.8, emissions of unburned hydrocarbons did not exceed 10 ppm C anywhere across the diameter.

Carbon Monoxide Emissions

Carbon monoxide emissions are expressed as ppmv in figure 9, and as emission index in figure 10. At military power, the CO emissions are relatively uniform across the exhaust. At Mach 2.0 the CO emission index is approximately 3, and decreases with increasing flight speed to approximately 1.5 at Mach 2.8. In afterburning modes, CO emissions are substantially higher than at military power for all flight speeds. The regions of the exhaust in which CO emissions are highest appear to be very dependent on afterburning power level. At minimum afterburning CO emissions are high in the center region where unburned hydrocarbon emissions are also high, although the high CO region is typically wider than the high unburned hydrocarbon region. At intermediate afterburning, the CO emissions at larger radii ($R/R_8 > 0.5$) are slightly greater than at minimum afterburning; see figures 9 and 10.

At maximum afterburning, CO emissions are high at radii near $R/R_8 \doteq 0.7$. This is not unexpected since the local fuel-air ratio (fig. 4) is near stoichiometric at this radius, and the equilibrium CO concentration would be on the order of 2 percent. For Mach 2.0, the CO is also high in the center region, but for Mach 2.4 the center region CO is less than at larger radii, and at Mach 2.8, CO is very low in the center.

In general, CO emissions decrease with increasing flight speed consistent with the higher pressures and temperatures in the combustion system at higher flight speeds.

Carbon Dioxide Emissions

In figure 11, the emission index profiles for carbon dioxide are shown for Mach 2.0, 2.4, and 2.8. These figures provide a composite picture of where inefficiencies occur during afterburning. For all flight speeds, the CO_2 emission indices decrease in the center, as a consequence of high CO, high HC, or in most cases, both. In general, afterburning efficiency in this region improves with increasing power level, as well as with increasing flight speed. At maximum afterburning, the CO_2 emission indices decrease at radii near 0.7 of the exhaust nozzle radius. As can be seen from the HC and CO profiles, figures 8 and 10, respectively, this decrease in CO_2 for larger radii is almost entirely a result of high carbon monoxide.

SUMMARY OF RESULTS

Gaseous emissions from a J-58 afterburning turbojet engine were measured at simulated flight conditions of Mach 2.0, 2.4, and 2.8 at 19.8 km altitude. For each flight condition, detailed profile measurements were made for four engine power levels from military through maximum afterburning. These measurements were made on a single diameter at the engine primary nozzle using a single point traversing gas sample probe.

The emissions profiles, presented in terms of concentration (ppmv) and emission index (g emittant/kg fuel) gave the following results.

1. In afterburning modes there are significant gradients in exhaust temperature, local fuel air ratio, and species concentrations across the exhaust plane. It was found that traverse increments on the order of 0.1 of the exhaust radius were required to document these gradients.

2. Oxides of nitrogen emissions increase by slightly more than a factor of two from Mach 2.0 to 2.8. The NO_x emission index values for military power at Mach 2.0, 2.4, and 2.8 indicate that the increase is nearly linear with increasing Mach number in this range.

3. For each flight condition the NO_x emission indices in afterburning modes are on the order of one-half of the value at military power for the same flight speed.

4. At military power, unburned hydrocarbon emission indices were less than 0.3 for all flight speeds.

5. In afterburning modes, hydrocarbon emissions were substantially higher than at military power due to high hydrocarbon concentrations in the center region of the exhaust. The peak concentrations and the radial extent of this region decreased with increasing flight speed and increasing power level.

6. The carbon monoxide emission index at military power for Mach 2.0 was approximately 3 g CO/kg fuel and decreased with increasing flight speed.

7. In afterburning modes, CO emissions were substantially higher than at military power for all flight speeds. The CO levels, and the regions of the exhaust in which these emissions are highest is very dependent on afterburning power level.

REFERENCES

1. Rudey, Richard A.; and Perkins, Porter J.: Measurement of High-Altitude Air Quality Using Aircraft. NASA TM X-68221, 1973.

2. Diehl, Larry A.: Preliminary Investigation of Gaseous Emissions From Jet Engine Afterburners. NASA TM X-2323, 1971.

3. Palcza, J. Lawrence: Study of Altitude and Mach Number Effects on Exhaust Gas Emissions of an Afterburning Turbofan Engine. NAPTC-ATD-212, Naval Air Propulsion Test Center (AD-741249; FAA-RD-72-31), 1971.

4. Diehl, Larry A.: Measurement of Gaseous Emissions from an Afterburning Turbojet Engine at Simulated Altitude Conditions. NASA TM X-2726, 1973.

5. German, R. C.; High, M. D.; and Robinson, C. E.: Measurement of Exhaust Emissions from a J85-GE-5B Engine at Simulated High-Altitude Supersonic Free-Stream Flight Conditions. ARO-PWT-TR-73-49, ARO Inc. (AD-764-717; AEDC-TR-73-103; FAA-RD-73-92), 1973.

6. Davidson, D. L.; and Domal, A. F.: Emission Measurements of a J93 Turbojet Engine. ARO-ETF-TR-73-46, ARO Inc. (AD-766648; AEDC-TR-73-132), 1973.

7. Procedure for the Continuous Sampling and Measurement of Gaseous Emissions from Aircraft Turbine Engines. Aerospace Recommended Practice 1256, SAE, Oct. 1971.
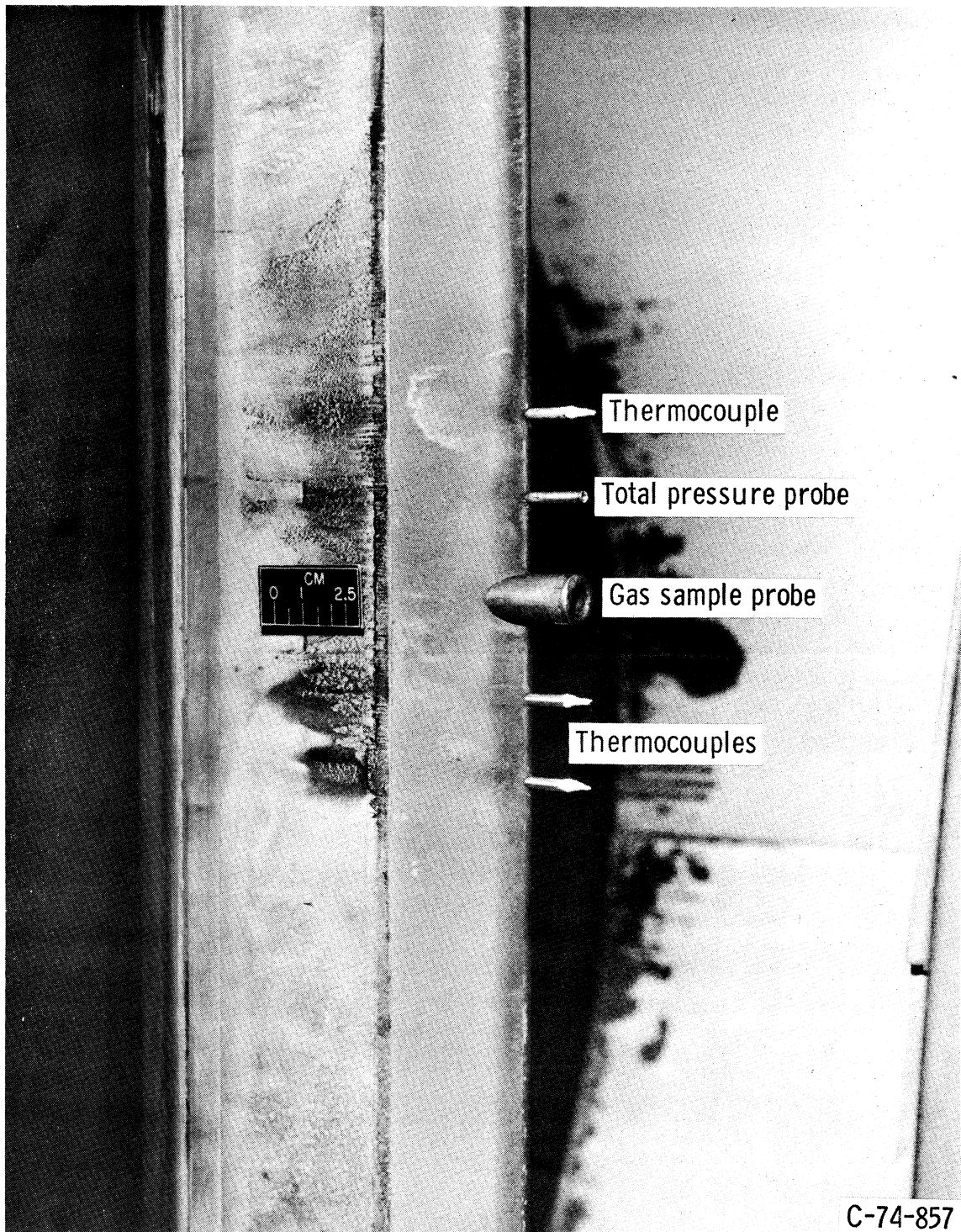
TABLE I. - TEST CONDITIONS

[Simulated altitude = 19.8 km]

	Mach number		
	2.0	2.4	2.8
Engine inlet temperature, K	390	465	553
Engine inlet pressure, atm	0.42	0.75	1.35
Altitude chamber pressure, atm	0.22	0.30	0.42
Military, f/a	0.018	0.015	0.013
Min A/B, f/a	0.042	0.037	0.033
Int A/B, f/a	0.050	0.044	0.040
Max A/B, f/a	0.064	0.059	0.057

Traverse mechanism

Gas sample probe

Engine exhaust nozzle
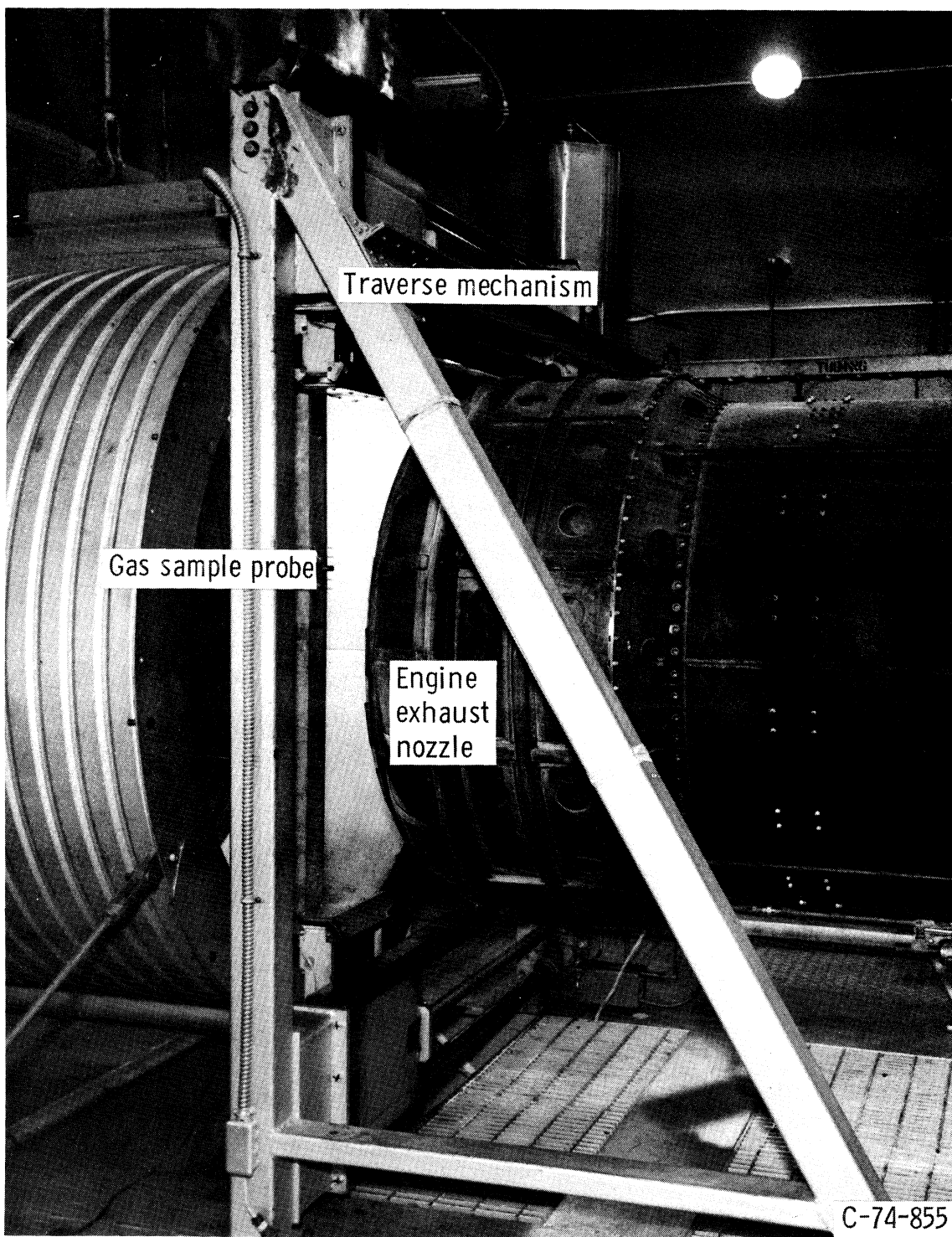
C-74-855

(a) Probe and traversing mechanism.

Figure 1. – Gas sample probe.

Thermocouple

Total pressure probe

Gas sample probe

Thermocouples

C-74-857

(b) Detail of sensor area.

Figure 1. – Concluded.

Figure 2. – Gas analysis console.
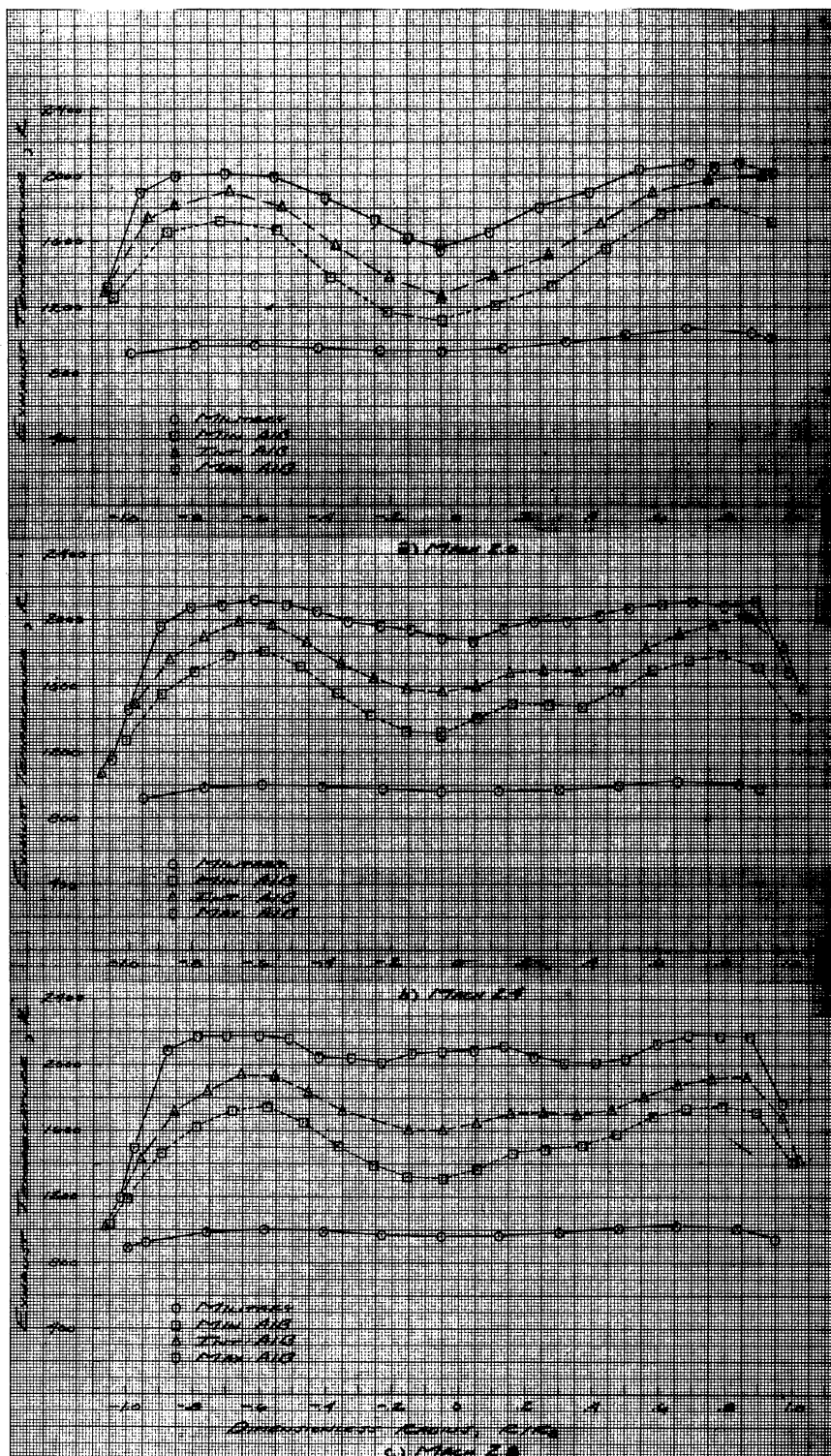
FIGURE 3. EXHAUST GAS TEMPERATURE
PROFILES. SIMULATED ALTITUDE, 19.8 KM

DIMENSIONLESS RADIUS, R/R_0

C) MACH 2.8
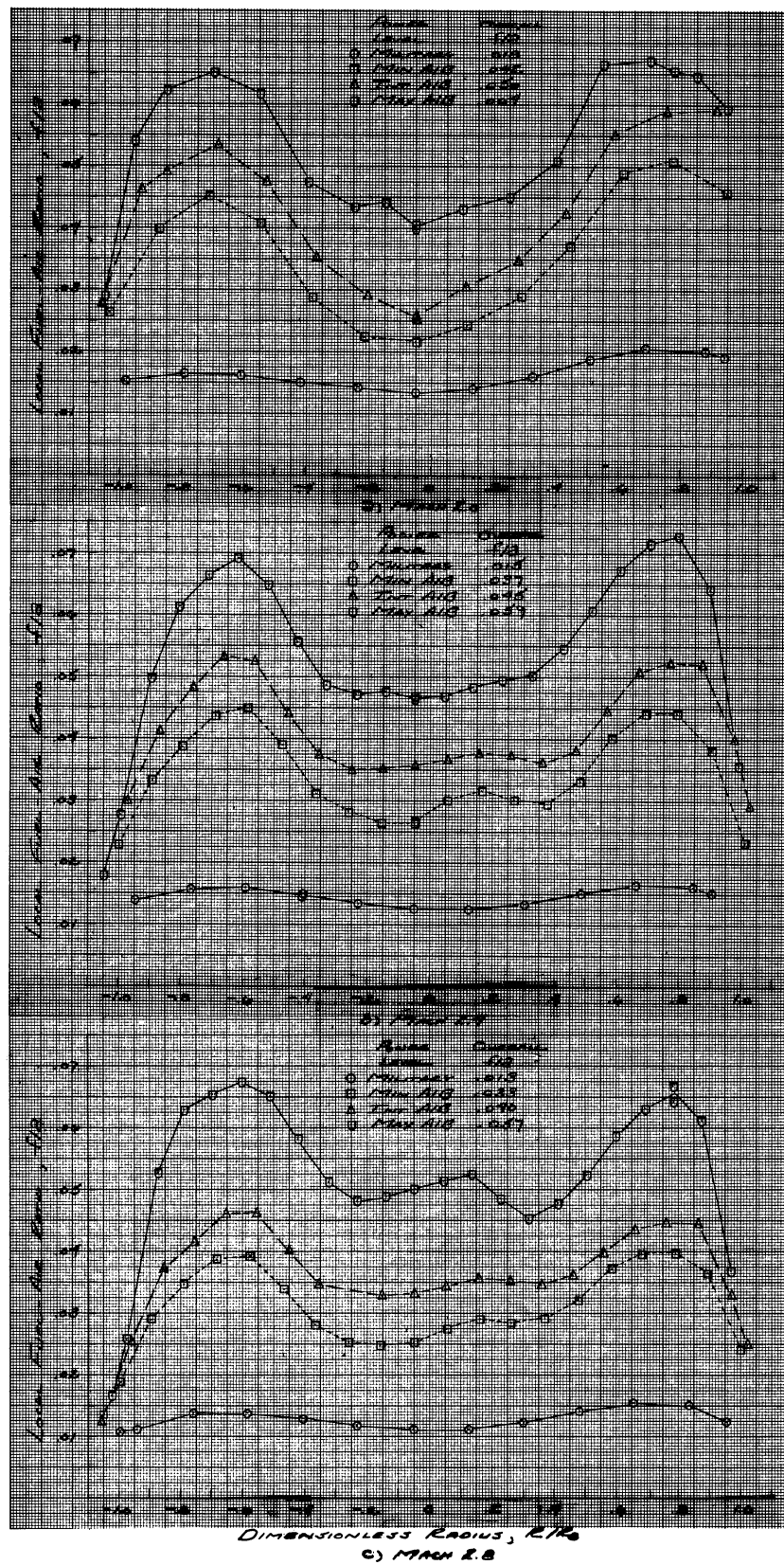
FIGURE 4. FUEL-AIR RATIO PROFILES.
SIMULATED ALTITUDE, 19.8 km
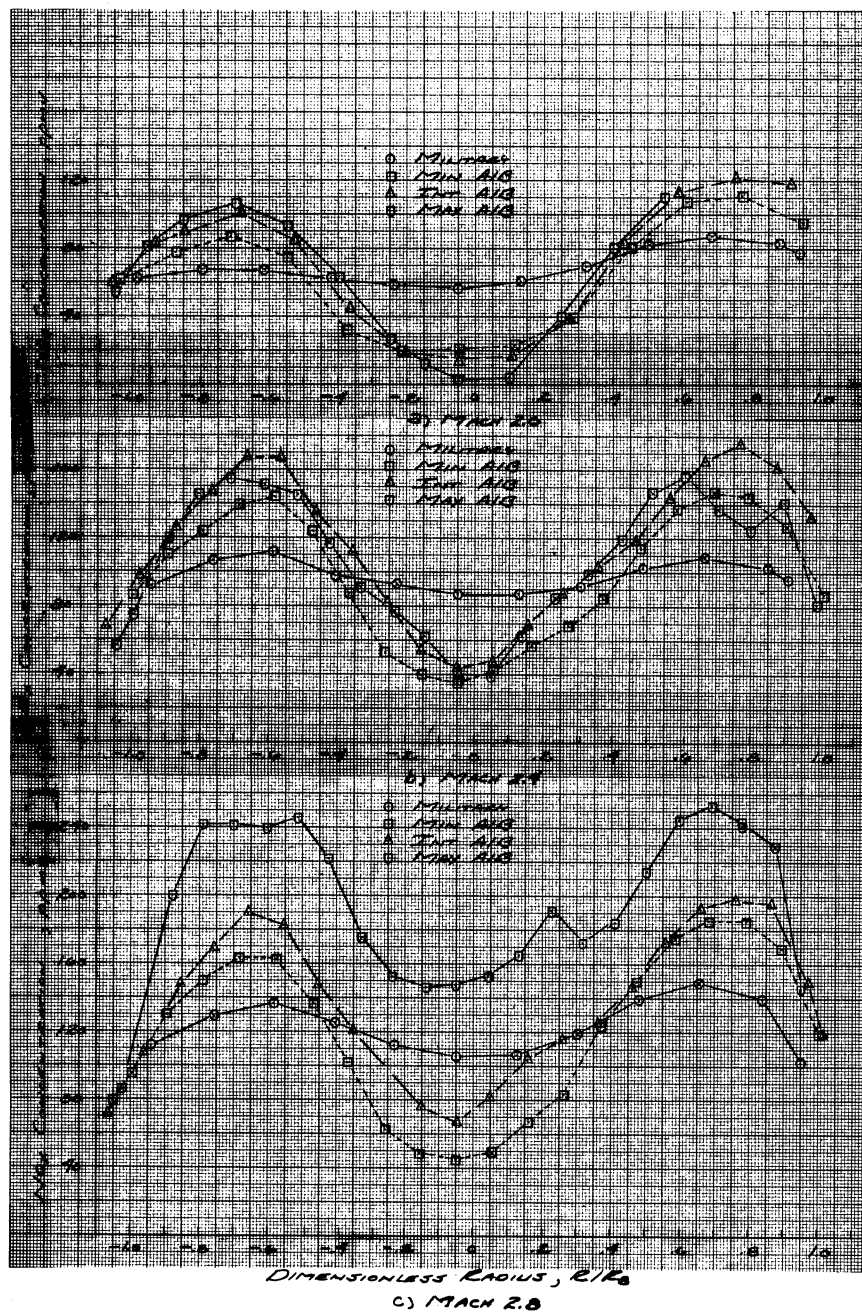
FIGURE 5 OXIDES OF NITROGEN CONCENTRATION
PROFILES. SIMULATED ALTITUDE, 19.8 KM.

DIMENSIONLESS RADIUS, R/R_o
C) MACH 2.8
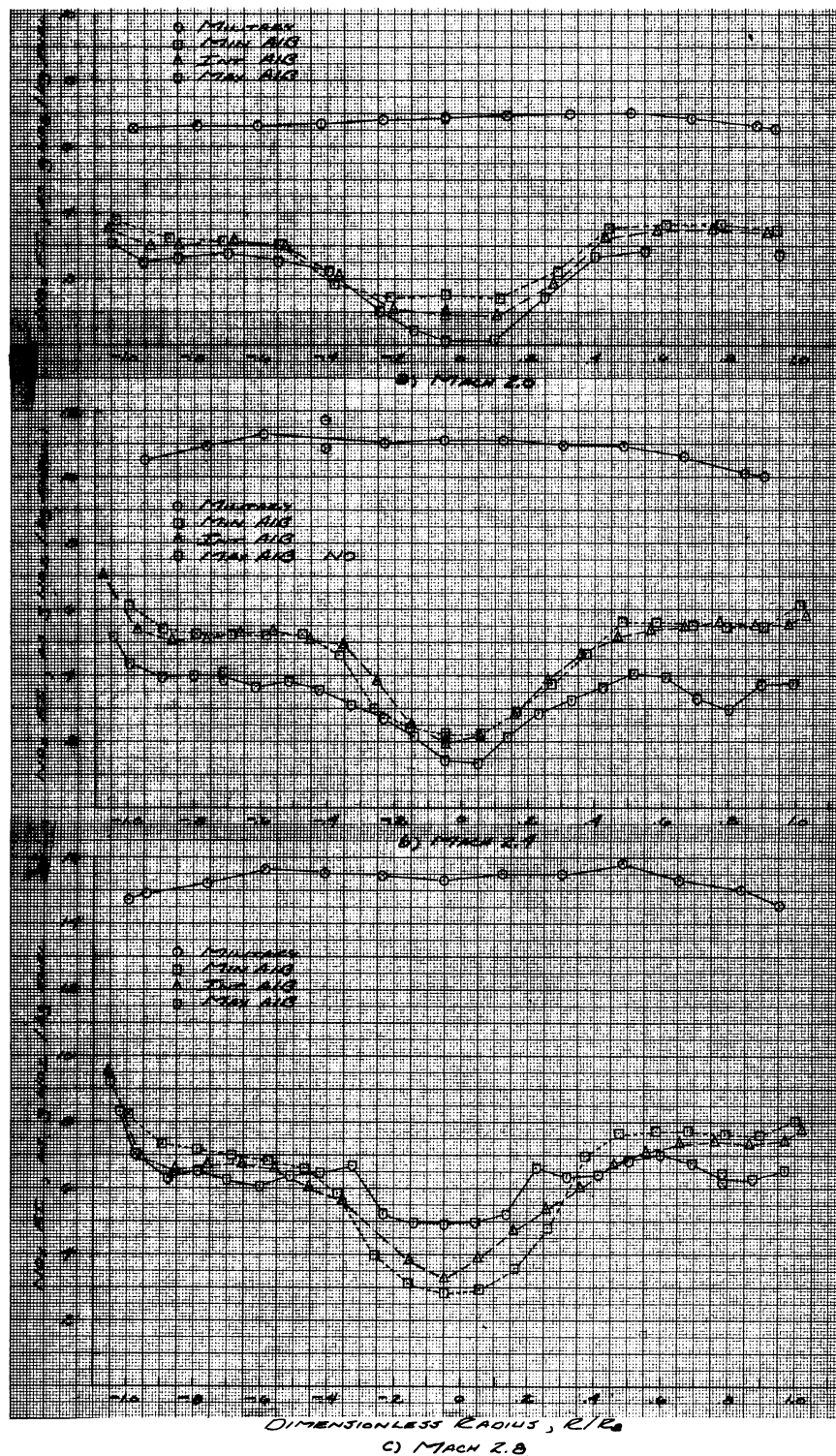
FIGURE 6. OXIDES OF NITROGEN EMISSION
INDEX PROFILES. SIMULATED ALTITUDE, 19.8 KM
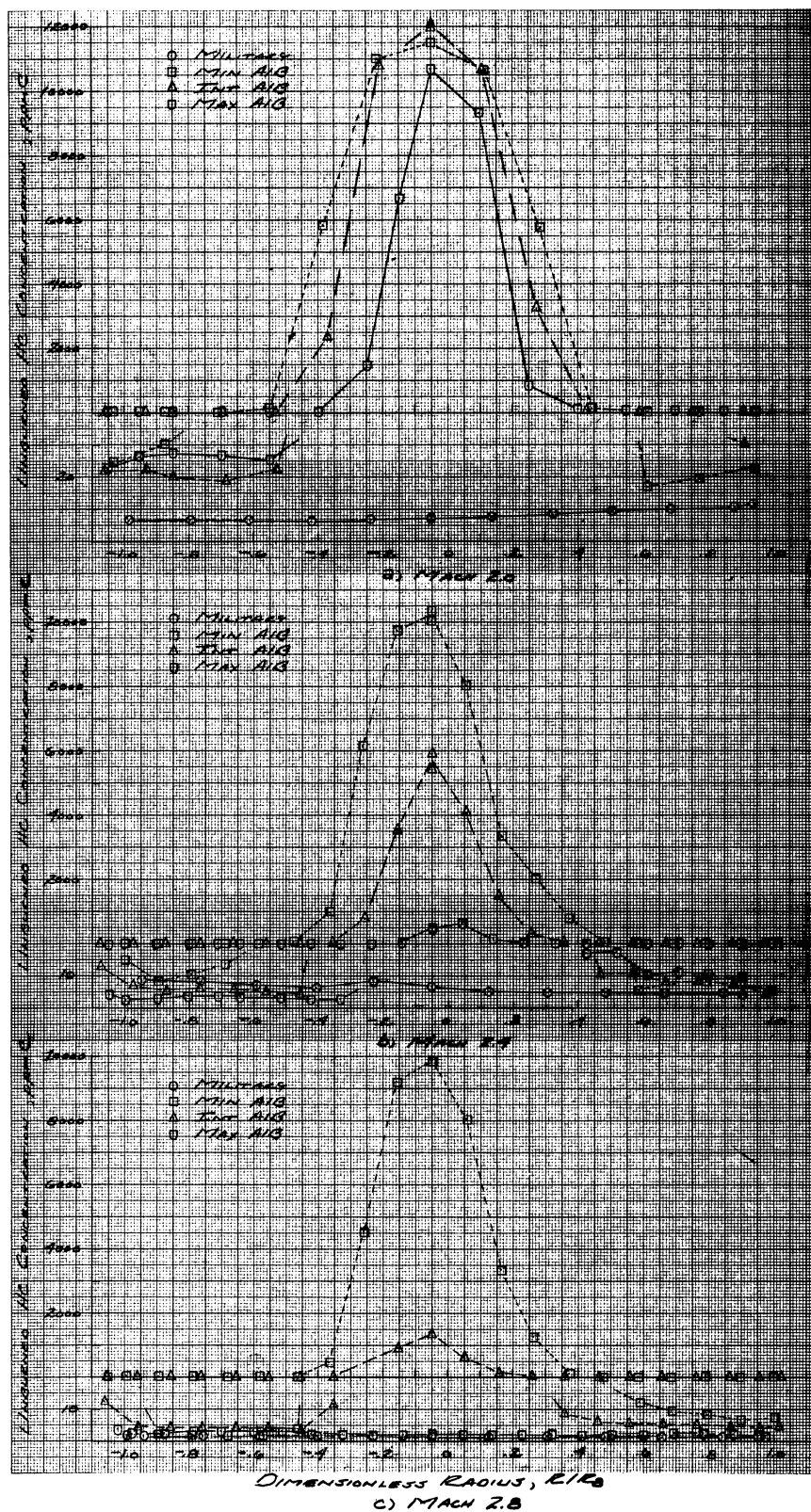
Figure 7. Unburned Hydrocarbons Concentration Profiles. Simulated Altitude, 19.8 km.
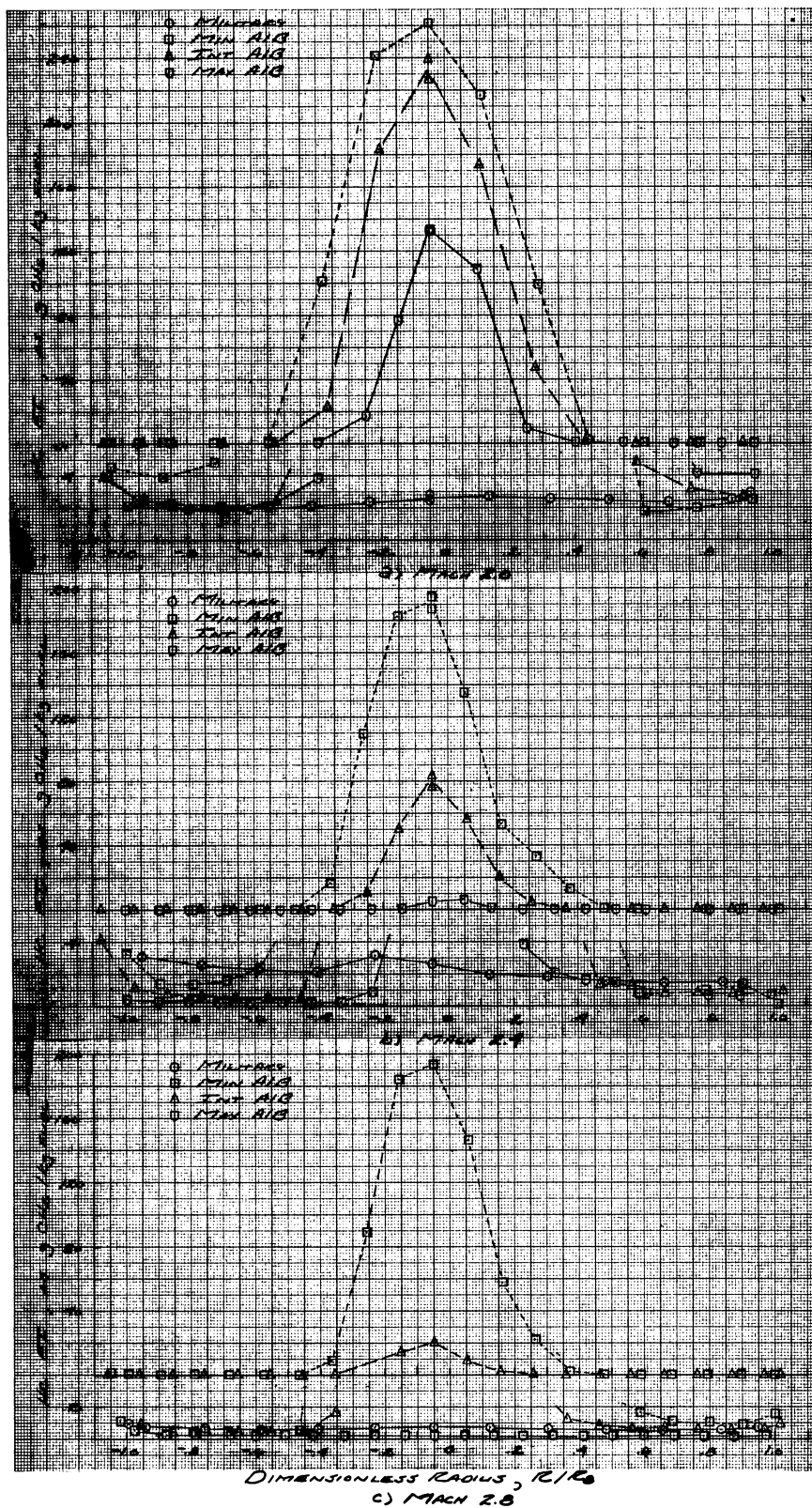
FIGURE 8. UNBURNED HYDROCARBONS EMISSION INDEX PROFILES. SIMULATED ALTITUDE, 19.8 KM

a) MACH 2.0
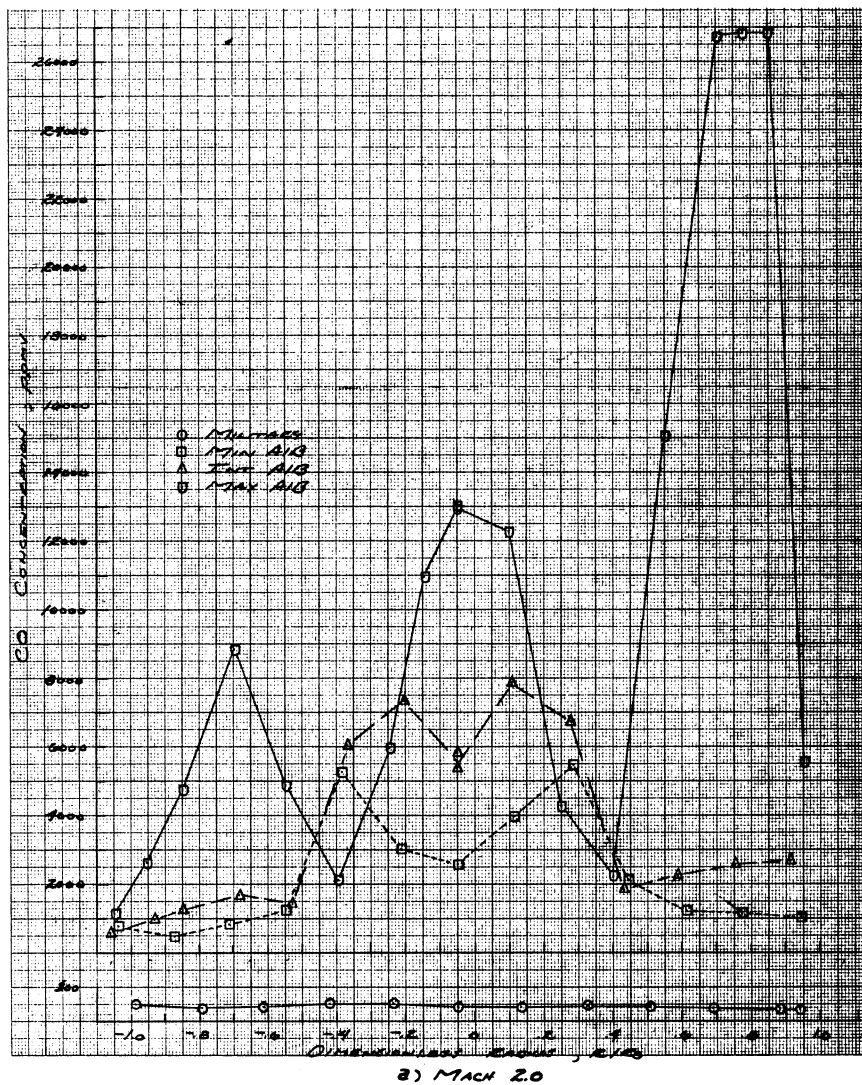
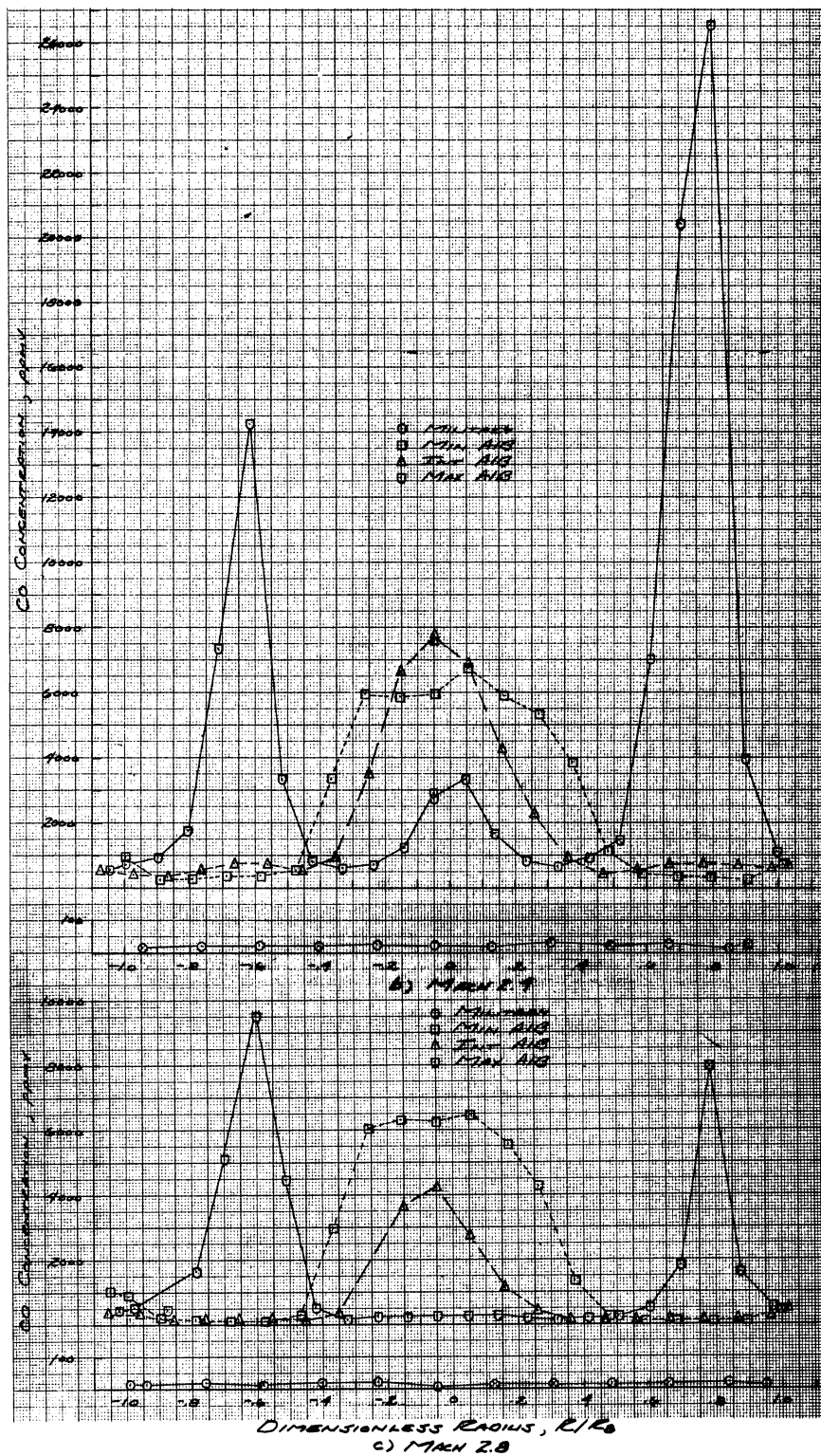FIGURE 9. CARBON MONOXIDE CONCENTRATION
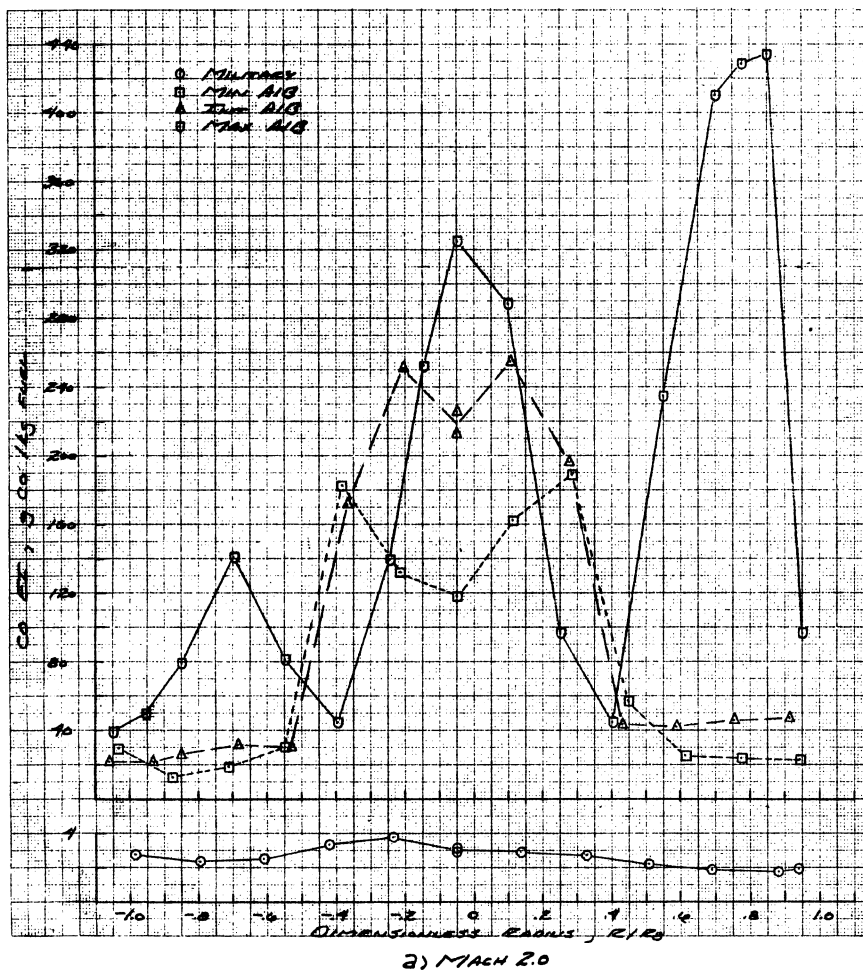PROFILES. SIMULATED ALTITUDE, 19.8 KM

Figure 9 Concluded

FIGURE 10. CARBON MONOXIDE EMISSION INDEX
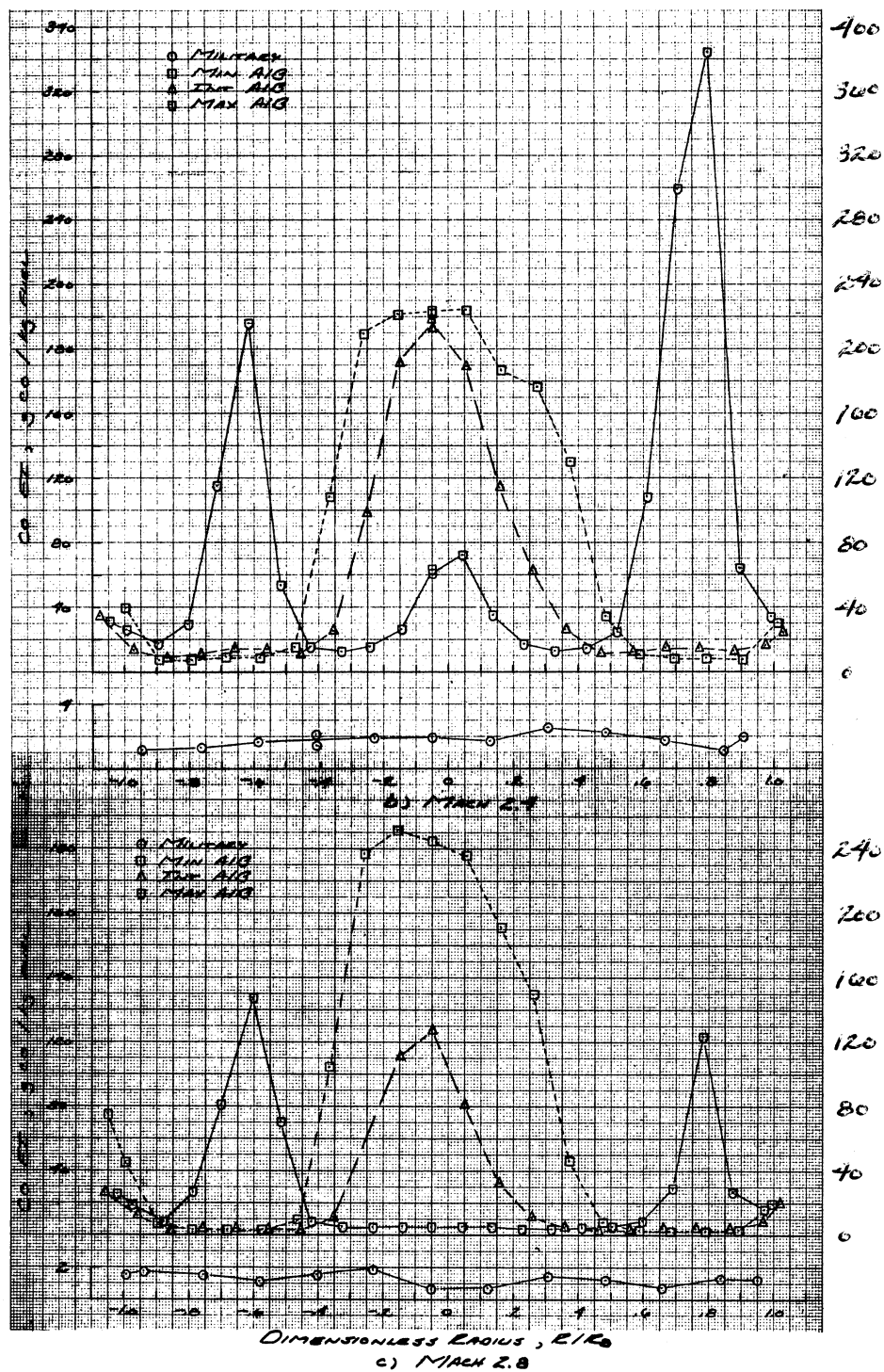PROFILES. SIMULATED ALTITUDE, 19.8 km

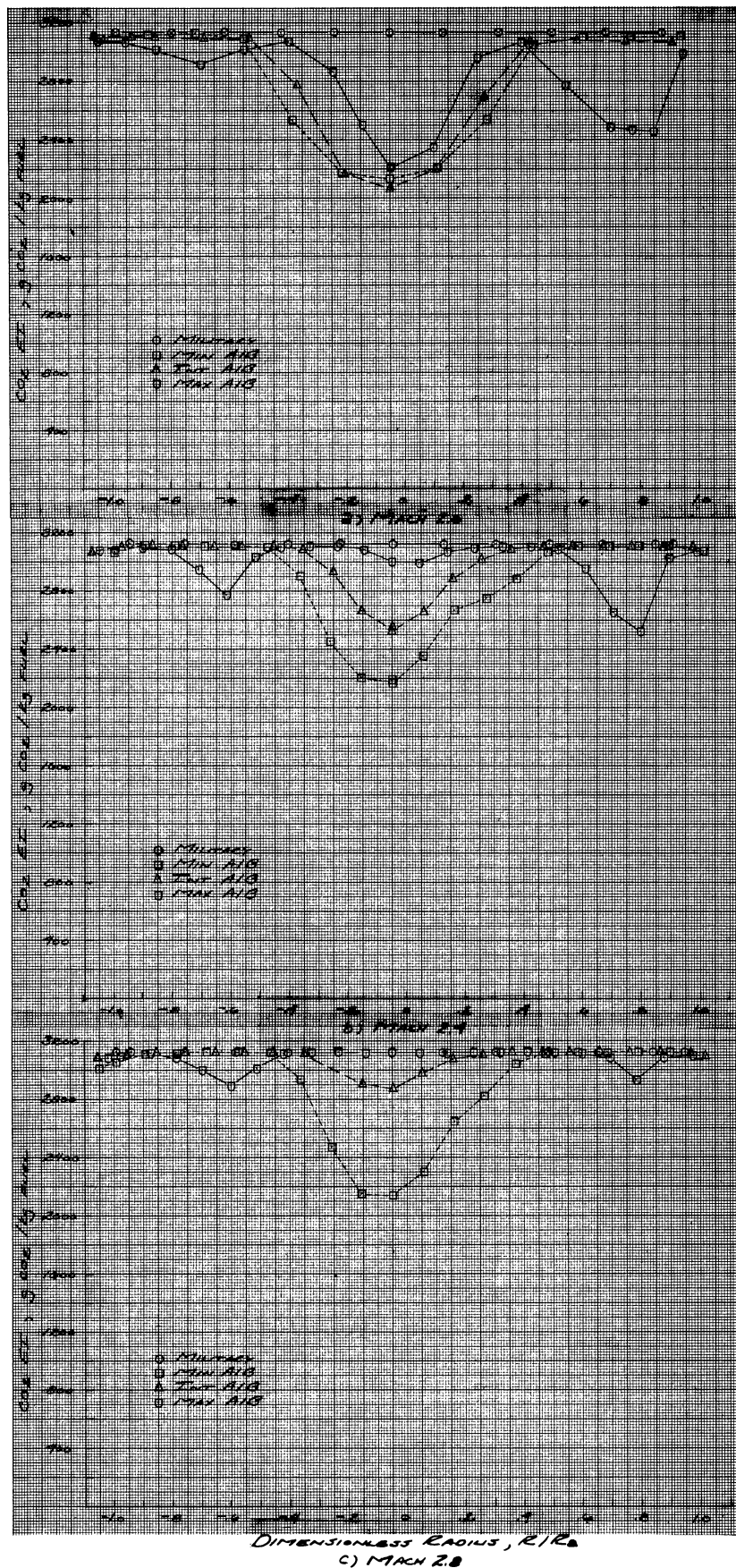DIMENSIONLESS RADIUS, R/R_o
c) MACH 2.8

FIGURE 10 CONCLUDED

Figure 11   Carbon Dioxide Emission Index
Profiles. Simulated Altitude , 19.8 km